Predicting pressure ulcer risk from seating interface pressure in people with spinal cord injury

Tim D. Yang · Yih-Kuen Jan

Abstract—The purpose of the study was to predict and visualize pressure ulcer risk in people with spinal cord injury (SCI). In conventional clinical practice, seating interface pressure assessments are based on summary statistics of pressure magnitude. In this study, a novel computational assessment was developed based on nonnegative matrix factorization (NMF) and stochastic gradient descent (SGD). Rank-2 NMF was applied to the seating interface pressure maps of loading and pressure-relieving conditions in 16 wheelchair users with SCI. The two NMF basis images encapsulated pressure concentration and pressure dispersion, respectively. The first basis converged on the ischial tuberosity under both seating conditions, whereas the second basis converged anterior to the ischial tuberosity during loading and converged on the coccyx during unloading. The SGD classification yielded 81.25% overall accuracy with a weighted F_1 score of 0.806. In general, higher ulceration risk was associated with higher and lower activations of the first and second bases, respectively. The NMF pipeline yielded promising performance. Basis visualization affirmed the importance of lower ischial pressure and higher distribution dispersion while also revealing that clinical practice may currently be underestimating the importance of coccygeal pressure in response to pressure-relieving activities.

Index Terms—Dimensionality reduction, Feature extraction, Nonnegative matrix factorization, Pressure ulcers, Prevention, Spinal cord injury, Visualization

1 Introduction

Feature extraction methods leverage dimensionality reduction to uncover latent patterns underlying the primitive data [1]. High-dimensional data are mapped into a low-dimensional feature space, which tends to yield computationally meaningful representations for classification, visualization, and compression [2]. However, computational meaning does not necessarily facilitate human interpretation. For example, the classical principal component analysis (PCA) imposes orthogonality and orthonormality constraints to generate eigenfeatures that can be easily interpreted statistically (i.e., as the directions of largest variance) but not visually, whereas the more recent nonnegative matrix factorization (NMF) imposes nonnegativity constraints to generate additive features that can be easily interpreted visually [1, 3]. Thus, PCA yields holistic basis images that tend to be more abstract, whereas NMF yields localized basis images that tend to be more intuitive. This characteristic makes NMF particularly amenable to image processing applications, such as facial recognition and medical imaging [4]. However, uses of NMF for medical imaging have yet to be fully explored, including applications for pressure ulcer prevention. Despite pressure ulcers becoming a healthcare priority in the US [5], pressure ulcer-related hospitalizations increased by 80% from 1993 to 2006 [6], whereupon treatment entailed $16,800 per hospitalization and $11 billion per year [7]. Approximately 60,000 people die each year from pressure ulcer complications in acute care [8]. Novel computational methods can help to combat this persistent healthcare challenge.

Quantitatively, hemodynamic properties have been investigated in relation to pressure ulcer risk. Hypotension has been associated with an increase in pressure ulcer risk due to decreases in skin perfusion and post-occlusive reactive hyperemia [9]. However, localized blood pressure (e.g., at vulnerable sites) cannot be reliably predicted from systemic blood pressure given the nonlinear decrease of blood pressure throughout the vascular tree. Furthermore, capillary blood pressure cannot be reliably predicted from seating interface pressure given the nonlinear transfer of interface pressure to internal pressure. Nevertheless, capillary closure pressure has historically been used as a proxy threshold for seating interface pressure [10]. The closure value of 32 mmHg [11] has been widely referenced despite being revised to 45 mmHg in follow-up work [12]. Moreover, the value was not measured under the ischial tuberosity but rather the nail fold and thus likely cannot be extrapolated to the ischial tuberosity since soft tissue and microvascular mechanics are dependent on local bone, muscle, and skin structure [13]. Despite these limitations, capillary closure pressure is still sometimes cited as an interface pressure threshold [10]. In practice, immersion (i.e., sinking depth) and envelopment (i.e., surface conformity) are pursued to decrease interface pressure at the bony prominences [14]. Support surfaces are assessed and prescribed by relative efficacy rather than absolute thresholds [15]. Thus, current clinical interventions and research methods are primarily based on pressure magnitude features. Work has been ongoing to determine reliable variables [16] and parameters [17, 18] for analyzing interface pressure magnitudes. Meanwhile, pressure ulcer incidence and prevalence remain excessive. Alternative analyses such as computational feature extraction may reveal hidden information not directly obtainable from conventional pressure magnitude

Manuscript received 18 Jan. 2019; accepted 12 Nov. 2019; published 12 Dec. 2019; issued Jan. 2020. This work was supported in part by the National Institutes of Health under Grant R03HD060751.

T. D. Yang (tyang15@illinois.edu) and Y.-K. Jan (yjan@illinois.edu) are with the Department of Kinesiology and Community Health, Program in Computational Science and Engineering, and Rehabilitation Engineering Laboratory at the University of Illinois Urbana-Champaign, Urbana, IL 61801 USA.

Digial Object Identifier 10.1007/s11517-019-02081-z

analyses.

Qualitatively, vigilant skin monitoring is performed to minimize pressure ulcer risk, for example, using the Braden scale of sensation, moisture, activity, mobility, nutrition, and friction. However, Braden scores are not strongly predictive of pressure ulcer development [19]. When skin breakdown occurs, skin integrity is graded according to the National Pressure Ulcer Advisory Panel (NPUAP) staging system [20]. Accordingly, early detection relies on the presentation of pain, which is limited or absent in clients with SCI [5]. Visual detection also relies on skin discoloration, which may be masked in clients with darker skin pigmentation [21]. These situations highlight the potential utility of computational feature extraction in predicting and detecting pressure ulcers. Computationally extracted features need not rely on pain presentation or skin pigmentation, which could potentially facilitate computational determination of skin integrity from seating interface pressure. Well-engineered features may reveal a feature space highly discriminative of ulceration status.

As such, existing quantitative and qualitative approaches to seating interface pressure assessment can be augmented by computational feature extraction methods such as NMF. The NMF method is especially well suited because it facilitates not only computational discrimination but also visual interpretation. Quantitatively, NMF yields a low-dimensional feature space within which pressure ulcer risk can be computed. Qualitatively, NMF yields basis images that may offer clinical insights to guide clinical seating pressure assessment (i.e., highly activated basis regions may reveal regions previously undervalued by clinical practice). The NMF method takes a nonnegative input matrix and yields two nonnegative factors,

$$\mathbf{V} \approx \mathbf{WH} \tag{1}$$

where the nonnegative input matrix $\mathbf{V}$ of m observations and n variables is decomposed into a nonnegative feature matrix $\mathbf{W}$ of r basis vectors and a nonnegative activation matrix $\mathbf{H}$ of r encoding weights,

$$\mathbf{V} \in \mathbb{R}_{\geq 0}^{m \times n} \tag{2}$$

$$\mathbf{W} \in \mathbb{R}_{\geq 0}^{m \times r} \tag{3}$$

$$\mathbf{H} \in \mathbb{R}_{\geq 0}^{r \times n} \tag{4}$$

The factors $\mathbf{W}$ and $\mathbf{H}$ can be iteratively constructed by optimizing the squared Frobenius norm between $\mathbf{V}$ and $\mathbf{WH}$ [1],

$$f(\mathbf{V} \mid \mathbf{WH}) = \frac{1}{2} \|\mathbf{V} - \mathbf{WH}\|_F^2 \tag{5}$$

Due to the global nonnegativity constraint, these resultant basis vectors in $\mathbf{W}$ are additive and thus amenable to semantic interpretability [1]. In this study, NMF was used to extract features from the seating interface pressure maps of people with SCI. The seating interface pressure maps were factorized into nonnegative basis images to visualize and predict pressure ulcer risk.

2 Methods

2.1 Participants

Power wheelchair users with SCI were recruited from a local rehabilitation hospital. Prospective participants were included if they (a) had sustained a traumatic SCI in the low-cervical and thoracic sections (i.e., between the levels of C4 and T12) at least 6 months prior to the experiment and (b) used a power wheelchair with a seat width of 43–53 cm as the primary means of mobility. The injury levels were chosen as a balance between neurophysiological homogeneity and pragmatic recruitment benchmarks. The 6-month injury window ensured that each participant's neurological state had stabilized by the time of the experiment. The seat width requirement ensured that each participant could reasonably fit in the laboratory power wheelchair used for the experiment. Participants were excluded if they had active pressure ulcers, cardiovascular diseases, or skeletal deformities (e.g., hip and knee contracture, pelvic obliquity, or scoliosis).

The recruited participants ($n = 16$) included 3 women and 13 men with 3 Black Americans, 1 Asian American, 1 Hispanic American, 1 multiracial American, and 10 Caucasian Americans. There were 3 complete and 13 incomplete injuries with 5 at the cervical level and 11 at the thoracic level. The mean age was 38.5 years (SD = 11.1), mean body weight was 78.7 kg (SD = 16.7), mean body mass index was 24.5 $\text{kg}\cdot\text{m}^{-2}$ (SD = 3.6), and mean duration of injury was 7.0 years (SD = 6.8). All participants gave informed consent to this study, which was approved by the local ethics committee (#14448).

2.2 Instrumentation

Seating interface pressure values were recorded with a flexible CONFORMat 5330 interface pressure mat [22] with a thickness of 0.762 cm. The mat contained 1024 sensels arranged in a 32×32 matrix with a sensel resolution of 0.5 cm^2. The mat system was calibrated prior to each recording session. A C300 power wheelchair [23] with a seat width of 48 cm, and the default high-density precontoured foam cushion was used across all recordings.

2.3 Data collection

Seating interface pressure maps from two configurations of wheelchair tilt (i.e., changing the seat-to-ground angle while maintaining the seat-to-back angle) and wheelchair recline (i.e., maintaining the seat-to-ground angle while changing the seat-to-back angle) from previous studies on skin perfusion response to tilt and recline were extracted for secondary analysis [24, 25, 26, 27]. The first configuration was the maximal loading configuration, which referred to the 0° tilt and 0° recline baseline posture. The second configuration was the maximal unloading configuration, which referred to the 35° tilt and 30° recline recovery posture. Both tilt and recline maneuvers were operated exclusively in the backward direction.

2.4 Data analysis

The baseline location of the right ischial tuberosity (i.e., under maximal loading) was used to align all pressure maps (i.e., under both loading conditions). Because the pressure maps were shifted by different directions and magnitudes, the alignment reduced the overlap between all pressure maps and limited the effective dimensions. Thus, the aligned pressure maps were cropped to a 24×14

window encompassing the right thigh and buttocks. The preprocessing yielded data in which the location of the right ischium varied under maximal unloading due to individual differences in sliding displacement from wheelchair tilt and recline [17]. These individual differences were preserved since they could potentially hold relevant information for the factorization.

Dimensionality was reduced as in (1). The nonnegative input matrix (2) contained $m = 16$ participants and $n = 24 \times 14 \times 2 = 672$ sensels and was decomposed into a nonnegative feature matrix (3) of $r = 2$ basis vectors and a nonnegative activation matrix (4) of $r = 2$ encoding weights. These bases were first visualized as individual images and subsequently superimposed as 90% contours on pressure maps of interest.

To bridge the results with clinical practice, two reliable clinical variables were referenced. The peak pressure index (PPI) refers to the mean pressure within a 9–10 cm^2 area of the ischial tuberosity [17, 28],

$$p_{\text{PPI}} = \frac{1}{n}\mathbf{1}^{\mathsf{T}}\mathbf{t} \tag{6}$$

$$\mathbf{t} \in \mathbb{R}^{n\times 1} \tag{7}$$

where $\mathbf{t}$ is the pressure n-vector under the ischial tuberosity and $\mathbf{1}$ denotes the ones vector. The dispersion index (DI) refers to the percentage pressure contained within the bony prominences (i.e., ischial and coccygeal regions) relative to the pressure map [28],

$$p_{\text{DI}} = \frac{\mathbf{1}^{\mathsf{T}}\mathbf{b}}{\mathbf{1}^{\mathsf{T}}\mathbf{a} + \mathbf{1}^{\mathsf{T}}\mathbf{b}} \tag{8}$$

where $\mathbf{b}$ is the pressure vector under the bony prominences and $\mathbf{a}$ is the pressure vector apart from the bony prominences. The Mann-Whitney U and Hedges' effect size g were used to compare PPI and DI between the predicted ulceration and nonulceration groups. The Mann-Whitney U test is a nonparametric hypothesis test to compare the difference between two independent samples. Hedges' g is a measure of the effect size for the difference between those samples' means.

Both the NMF and clinical analyses were performed using Python. The factorization and classification were implemented as a pipeline using built-in classes and functions from the scikit-learn machine learning library [29]. The pipeline included a standardization transformer, factorization transformer, and classification estimator. The standardization was implemented with unit variance scaling but without mean centering to preserve nonnegativity. The factorization was initialized with nonnegative double singular value decomposition [30] and solved with cyclic coordinate descent [31]. The classification was implemented as a linear estimator with a stochastic gradient descent learning function and a probabilistic loss function. Pressure ulcer risk was represented as the estimated probability of pressure ulceration,

$$f(p, y) = \begin{cases} -4py & \text{if } py < -1 \\ (1 - py)^2 & \text{if } py \in [-1, 1) \\ 0 & \text{otherwise} \end{cases} \tag{9}$$

where p is a prediction and y is its corresponding label [32]. For model validation, a leave-one-out policy was applied to the analysis pipeline. For visualization, cubic spline interpolation was applied to the factorized basis images. The Mann-Whitney U test was implemented using scipy's built-in statistical functions. Hedges' g was computed with an adjustment for robustness against uneven group sizes and small sample sizes by weighting the pooled standardizer and applying a bias coefficient, respectively.

3 Results

The first NMF basis image encapsulated pressure concentration, whereas the second NMF basis encapsulated pressure dispersion (Figure 1). Points of convergence were visualized by overlaying 90% contours of the NMF bases onto the mean pressure maps of maximal loading and maximal unloading (Figure 2). The first NMF basis converged on the ischial tuberosity under both loading conditions. The second NMF basis image converged anterior to the ischial tuberosity under maximal loading and converged on the coccyx under maximal unloading.

After projecting the data onto the NMF feature space (Figure 3), the study sample was classified with an overall accuracy of 81.25% and a weighted F_1 score of 0.806. The area under the receiver operating characteristic curve was 0.754 (95% bootstrapped confidence interval: 0.626–0.882), and the area under the precision-recall curve was 0.750 (95% bootstrapped onfidence interval: 0.561–0.917).

In general, higher ulceration risk was associated with higher activation of the first NMF basis (i.e., higher ischial pressure) and lower activation of the second NMF basis (i.e., lower pressure dispersion) (Figure 4). Overall, the classification yielded three errors: one false positive (Figure 5) and two false negatives (Figure 6).

Under maximal loading, PPI and DI respectively increased by a significant 127.9% ($U(14) = 3.00$, $p < .01$, $g = 2.04$) and a significant 28.8% ($U(14) = 4.00$, $p < .01$, $g = 1.84$) when comparing the predicted ulceration group to the predicted nonulceration group. Under maximal unloading, PPI and DI respectively increased by a significant 112.4% ($U(14) = 9.00$, $p < .05$, $g = 1.45$) and a significant 34.3% ($U(14) = 1.00$, $p < .01$, $g = 2.18$) when comparing the predicted ulceration group to the predicted nonulceration group.

4 Discussion

Given the profound physical, psychological, and financial consequences of pressure ulcers, prevention would reduce the cost of pressure ulcer care by more than 90% [33]. However, as evidenced by the persistently high rates of prevalence and incidence, the path to prevention remains unclear. Prevention commands lifelong vigilance from at-risk clients and clinicians, and current clinical practice relies heavily on subjective and surrogate measures to assess skin integrity and wound risk. Feature extraction could supplement clinical practice with a computational method for visualizing and predicting pressure ulcer risk. Counter to more black-box approaches whose intermediate components are abstract or hidden, NMF exposes visually interpretable basis images. The factorization further generates a feature space in which pressure ulcer risk can be computed. Combined,

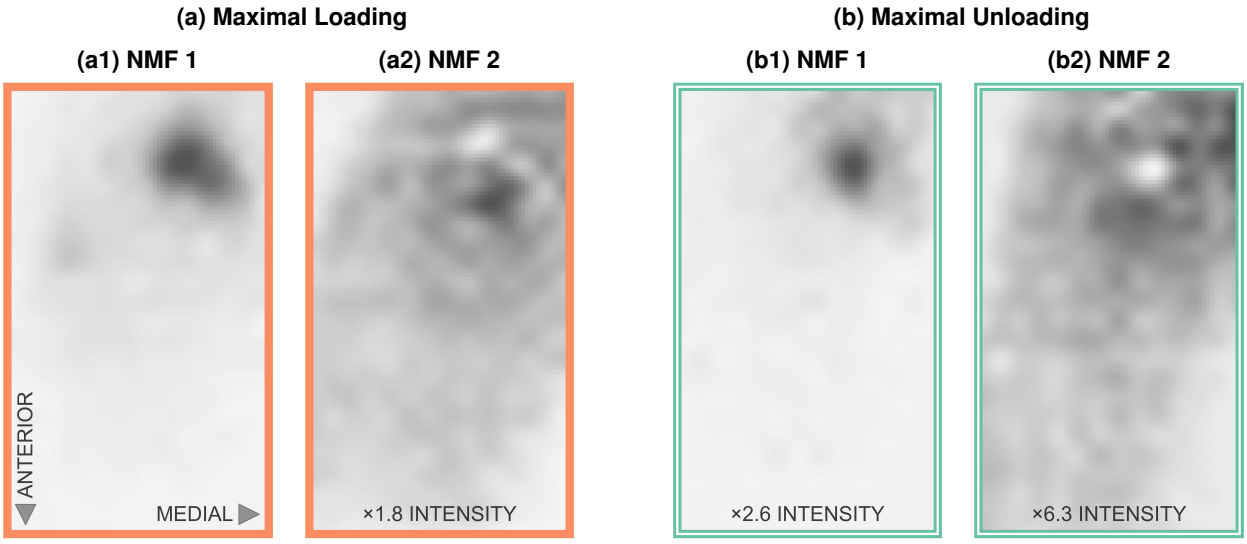

Fig. 1: Nonnegative matrix factorization (NMF) basis images of the right buttock: NMF 1 under maximal loading (a1), NMF 2 under maximal loading (a2), NMF 1 under maximal unloading (b1), and NMF 2 under maximal unloading (b2).

the analysis pipeline yields clinical implications for pressure ulcers through visualization and prevention.

4.1 Visualization

The NMF basis images highlighted the most relevant characteristics of seating interface pressure and captured clinical intuition on both distribution and magnitude characteristics. Reenalda et al. [34] systematically reviewed studies in which (a) interface pressure was a predictive or prognostic factor and (b) pressure ulcer development or healing was an outcome measure. Four studies investigated the seated posture, drawing clinical conclusions on the relationship between the pressure interface and pressure ulcers with respect to distribution [35] and magnitude [15, 36, 37].

4.1.1 Pressure distribution

Drummond et al. [35] measured seating interface pressure in 16 people with paraplegia between the high-lumbar and thoracic levels. Ischial and coccygeal loading were posteriorly redistributed in the ten participants with ulceration versus the six without ulceration. Within the thoracic injury group, the anteroposterior distribution was a discriminating factor between ulceration and nonulceration: Those with thoracolumbar kyphosis had a more anterior seating distribution and did not develop ulcers, whereas those with a straight lumbar had a more posterior distribution and developed ulcers. The more anterior distributions offloaded at-risk regions of the ischia and coccyx and may have consequently lowered the risk of ulceration. Clinically, this principle is quantified using DI, such that higher DI values suggest higher injury risk through lower pressure dispersion [28, 38]. Drummond et al. [35] proposed that a 55% DI may be reasonable as an injury risk threshold based on their study sample; however, conclusive thresholds are yet to be generalized.

In this study, the NMF results both affirmed existing intuition and revealed new insights on pressure dispersion. Existing intuition was affirmed when lower dispersion was associated with increased pressure ulcer risk. In the maximal loading posture, interface pressure under the thigh region was lower in the predicted ulceration group (Figure 4a1), yielding a significant 28.8% increase in DI versus the predicted nonulceration group (Figure 4a2). The first NMF basis converged on the ischial tuberosity, whereas the second NMF basis converged anterior to the ischial tuberosity and appeared to serve as a marker for anteroposterior dispersion. New insight was revealed when coccygeal pressure was associated with increased pressure ulcer risk. In the maximal unloading posture, the predicted ulceration group again presented with lower interface pressure under the thigh region (Figure 4b1), yielding a significant 34.3%

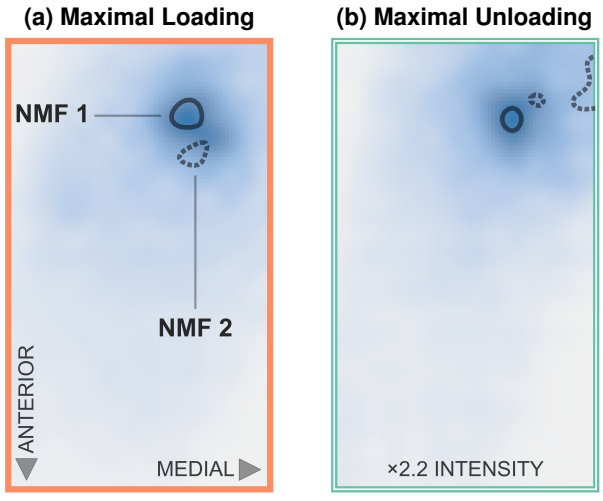

Fig. 2: Mean pressure maps of the right buttock during maximal loading (a) and maximal unloading (b) superimposed with 90% contours of the nonnegative matrix factors NMF 1 (solid) and NMF 2 (dotted).

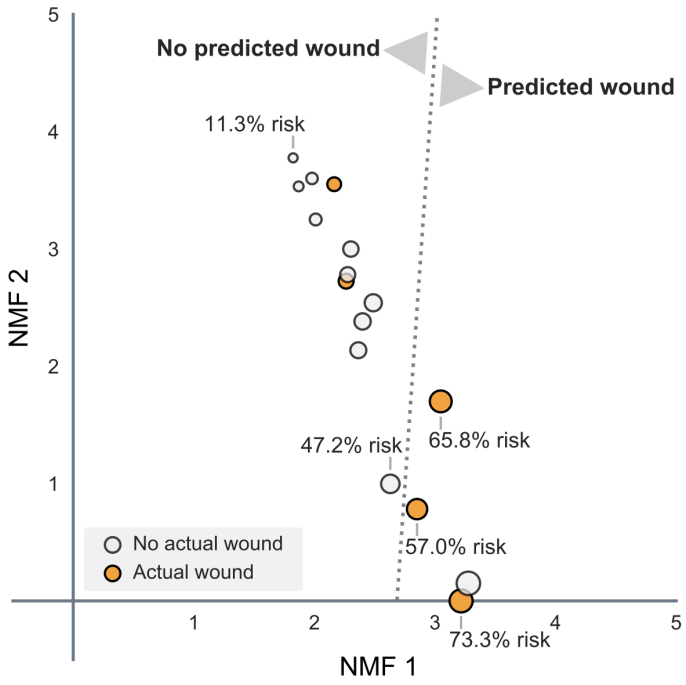

Fig. 3: Nonnegative matrix projection of participants with ulceration (filled) and nonulceration (unfilled) onto a stochastic gradient decision surface of predicted ulceration and predicted nonulceration; axis units in the projected space are arbitrary. Abbreviations: NMF (nonnegative matrix factorization)

increase in DI versus the predicted nonulceration group (Figure 4b2). The first NMF basis still converged on the ischial tuberosity, but the second NMF basis converged on the coccyx. Coccygeal pressure in response to wheelchair tilt and recline remains unclear. Giesbrecht et al. [39] found that coccygeal pressure monotonically decreased in response to wheelchair tilt. When combined with wheelchair recline, Chen et al. [40] found that coccygeal pressure initially increased in response to smaller angles of wheelchair tilt and only began decreasing at larger angles. The second NMF basis appeared to highlight the coccygeal in response to wheelchair tilt and recline, which has been markedly understudied relative to ischial pressure [40]. Thus, coccygeal pressure may warrant more focus in research and practice.

4.1.2 Pressure magnitude

Kosiak [41] first established a predictive relationship between pressure magnitude and pressure ulcer development in the laboratory setting. Governed by a reciprocal pressure-time relationship, low magnitudes over long durations are as harmful as high magnitudes over short durations. In real-world settings, tissue loading conditions are more dynamic than those of controlled experiments. Nevertheless, Conine et al. [36] and Brienza et al. [15] found a positive association between buttock-seat interface pressure and pressure ulcer incidence in at-risk elderly wheelchair users. Furthermore, Conine et al. [36] observed that ulceration incidence rose significantly when peak seating interface pressure exceeded 60 mmHg. However, predictive absolute thresholds could not be generalized.

Evidence has also suggested a prognostic relationship between lower pressure magnitude and faster pressure ulcer healing. Rosenthal et al. [37] conducted a randomized control trial comparing the healing rate of advanced pressure ulcers while sitting upright on a custom therapeutic seat cushion versus lying supine on a low air loss bed. The seat intervention was associated with lower interface pressure and with faster healing. However, the healing rate may have been confounded by an alternating pressure component of the therapeutic seat. Alternating the loading of compressed soft tissues is hypothesized to enhance wound healing by increasing skin perfusion and modulating the characteristic frequencies of skin blood flow oscillations in people with SCI [42, 43]. Thus, prognostic absolute thresholds also could not be generalized.

In this study, the NMF results offered affirmation of clinical intuition on pressure magnitude. In the maximal loading posture, PPI increased significantly by 127.9% in the predicted ulceration group (Figure 4a1) versus the predicted nonulceration group (Figure 4a2). In the maximal unloading posture, PPI increased significantly by 112.4% in the predicted ulceration group (Figure 4b1) versus the predicted nonulceration group (Figure 4b2). Thus, the NMF bases aligned with clinical intuition that seating interface pressure magnitude plays a key role in pressure ulcer risk.

4.2 Prevention

The NMF bases offered not only affirmation and revelation of clinical insights but also a potential means for pressure ulcer prevention. Computational detection would supplement clinical practice with an objective, systematic procedure for predicting pressure ulcer risk. For example, interface pressure-based computational detection could expose an early-stage ulcer that had otherwise escaped detection due to darker skin pigmentation; it could notify someone with SCI of an early-stage ulcer that had otherwise gone unnoticed due to impaired pain sensation; or it could simply serve as an additional criterion in borderline clinical cases.

In this study, the foundation was laid for such a computational detection pipeline (Figure 7):

1) factorize a training set of seating interface pressure maps from existing clients into NMF basis maps (Figure 7a),
2) project the training set into the factorized feature space and compute a probabilistic decision surface that accounts for each client's wound history (Figure 7b), and
3) project the pressure maps from clients of interest into the factorized feature space, within which their locations on the decision surface will reveal their corresponding wound probability (Figure 7c).

While the generated model in this study was likely overfitted due to the limited sample size, it provides a proof of concept for such a pressure ulcer prediction pipeline. In practice, this pipeline would require a larger sample size to yield meaningful predictions. Fortunately, pressure mapping is commonly used in clinical settings, although steps should be taken toward standardized data collection practices for more reliable model outcomes.

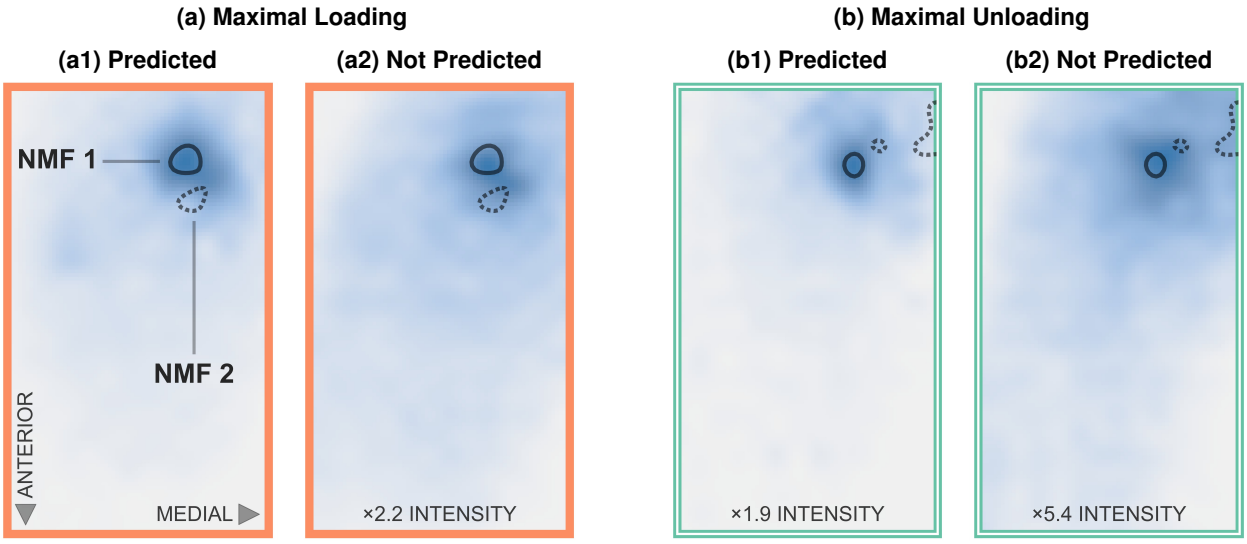

Fig. 4: Mean pressure maps of the right buttock from participants with and without predicted wound history superimposed with 90% contours of nonnegative matrix basis vectors NMF 1 (solid) and NMF 2 (dotted): predicted ulceration under maximal loading (a1), predicted nonulceration under maximal loading (a2), predicted ulceration under maximal unloading (b1), and predicted nonulceration under maximal unloading (b2).

The widespread clinical usage of pressure mapping supports the opportunistic screening of pressure maps for pressure ulcer risk. In the opportunistic screening paradigm, routine clinical data are leveraged for secondary analysis [44]. For example, osteoporosis and colorectal cancers are both detected using computed tomography (CT) via CT bone densitometry and CT colonography, respectively. Simultaneous screening of both conditions with a single CT scan limits the radiation and expenses incurred by clients and has thus prompted the automated computation of bone mineral density from existing CT colonography scans [45]. Likewise, automated computation of pressure ulcer risk from existing clinical pressure maps may enhance pressure ulcer prevention without adding much additional cost.

The widespread availability of interface pressure mapping further supports the feasibility of generating a sufficiently large database of labeled pressure maps to increase robustness against confounding cases. For example, the false positive in this study (i.e., predicted ulceration with actual nonulceration) may have been triggered by unique dispersion patterns (Figure 5). During loading (Figure 5a), there was a pressure void directly on the second NMF basis, while the remaining distribution was relatively dispersed. This unique dispersion pattern may have confounded the classification due to the low sample size. During unloading (Figure 5b), ischial pressure was dispersed laterally toward the trochanter rather than medially toward the coccyx and resulted in a relatively inactive second NMF basis. Although low activation of the second NMF basis (i.e., low coccygeal pressure) was generally indicative of higher ulceration risk (i.e., through lower dispersion), the unique lateral dispersion may have lowered the participant's wound risk. The false negatives (i.e., predicted nonulceration with actual ulceration) were more confounding and may not be explainable without future work. Qualitatively, their distribution and magnitude characteristics were not particularly indicative of high risk (Figure 6). Quantitatively, detectable features will likely require more training data. Factors such as pressure ulcer stage and quality of care were not available in this study. For example, the pressure ulcers of the false negatives may have been of a lower stage than that of the true positives. In future work, more detailed training data may yield a higher number of pertinent basis images and reveal additional discriminatory information in relation to ulceration risk.

Computational detection would also facilitate real-time monitoring of pressure ulcer risk. While constant clinical

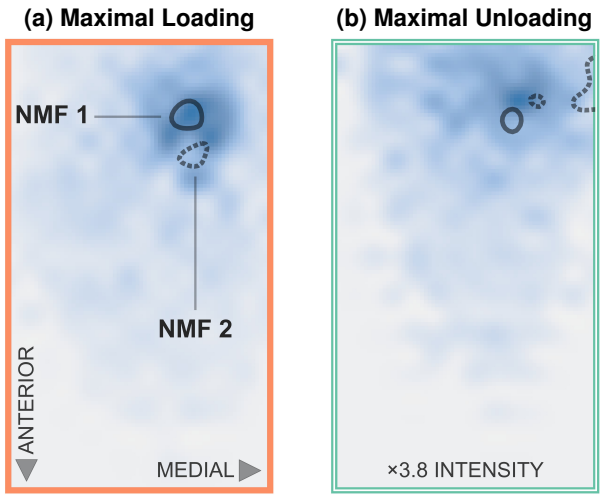

Fig. 5: Pressure maps of the right buttock from the lone false positive (i.e., predicted ulceration with actual nonulceration) during maximal loading (a) and maximal unloading (b) superimposed with 90% contours of nonnegative matrix basis vectors NMF 1 (solid) and NMF 2 (dotted).

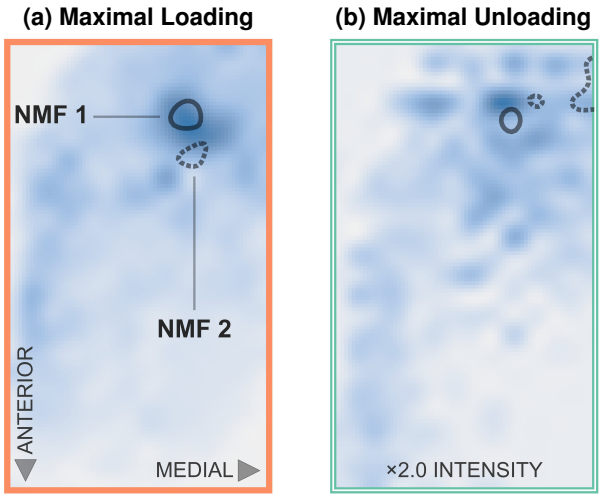

Fig. 6: Pressure maps of the right buttock from a false negative (i.e., predicted nonulceration with actual ulceration) under maximal loading (a) and maximal unloading (b) superimposed with 90% contours of nonnegative matrix basis vectors NMF 1 (solid) and NMF 2 (dotted).

monitoring is too costly to implement pragmatically [19], automated remote monitoring may be feasible. Several studies have investigated remotely monitoring pressure relief [46, 47, 48] and pressure distribution [49, 50]. The analysis pipeline in this study could be integrated into a real-time pressure monitoring system that periodically assesses in situ pressure maps against factorized pressure maps.

5 Limitations

This study was limited by its training data and study sample. Regarding the training data, the left half of the pressure maps was not available since the left ischial area had been modified for a separate study. Complete pressure distributions would likely yield more discriminatory information. On the right ischial tuberosity, there was a small, thin laser Doppler sensor to record skin perfusion for a previous study. Its effect on the analysis was minimal given the sensor's small size and systematic appearance throughout all pressure maps. In addition, wound history was based on self-reports rather than medical records and was labeled as ulceration versus nonulceration, lacking more precise details such as location, duration, and severity. The model also lacked other known risk factors, such as microenvironment conditions. Future training data could include the Braden subscores for a more comprehensive coverage of risk factors. Lastly, the data were collected on a standardized cushion, whereas the participants' natural cushions may have yielded improved classification performance.

Regarding the study sample, the sample size was low ($n = 16$). Furthermore, all participants were recruited from a single metropolitan area. Especially in the context of pattern recognition, a larger and more diverse sample would yield higher discrimination between classes. The model generated in this study was likely overfitted to the small sample. Given more training data and more precise class labels, the proposed analysis pipeline should be more generalizable and reveal more clinical insights.

6 Conclusions

This study leveraged a nonnegative factorization method for quantitative pressure ulcer prediction. Visualization of the interpretable factors affirmed the importance of lower ischial pressure and higher distribution dispersion while also revealing that current clinical practice may be underestimating the importance of coccygeal pressure in response to wheelchair tilt and recline. Given a larger set of training data, the method may reveal more clinical insights and higher predictive accuracy of pressure ulcer risk.

References

[1] Y.-X. Wang and Y.-J. Zhang, "Nonnegative matrix factorization: A comprehensive review," *IEEE Transactions on Knowledge and Data Engineering*, vol. 25, no. 6, pp. 1336–1353, 2013. DOI: 10.1109/tkde.2012.51.

[2] L. van der Maaten, E. Postma, and J. van den Herik, "Dimensionality reduction: A comparative review," Tilburg Centre for Creative Computing, Tilburg University, Technical Report TiCC-TR 2009-005, 2009, p. 36.

[3] D. D. Lee and H. S. Seung, "Learning the parts of objects by non-negative matrix factorization," *Nature*, vol. 401, pp. 788–791, 1999. DOI: 10.1038/44565.

[4] A. Sotiras, S. M. Resnick, and C. Davatzikos, "Finding imaging patterns of structural covariance via non-negative matrix factorization," *Neuroimage*, vol. 108, pp. 1–16, 2015. DOI: 10.1016/j.neuroimage.2014.11.045.

[5] E. A. Kruger, M. Pires, Y. Ngann, M. Sterling, and S. Rubayi, "Comprehensive management of pressure ulcers in spinal cord injury: Current concepts and future trends," *Journal of Spinal Cord Medicine*, vol. 36, no. 6, pp. 572–585, 2013. DOI: 10.1179/2045772313Y.0000000093.

[6] I. M. Jankowski and D. M. Nadzam, "Identifying gaps, barriers, and solutions in implementing pressure ulcer prevention programs," *Joint Commission Journal on Quality and Patient Safety*, vol. 37, no. 6, pp. 253–264, 2011. DOI: 10.1016/s1553-7250(11)37033-x.

[7] C. A. Russo, C. Steiner, and W. Spector, "Hospitalizations related to pressure ulcers among adults 18 years and older, 2006," in *Healthcare Cost and Utilization Project (HCUP) statistical briefs*. Rockville, MD: Agency for Healthcare Research and Quality, 2008, vol. 64.

[8] K. D. Duncan, "Preventing pressure ulcers: The goal is zero," *Joint Commission Journal on Quality and Patient Safety*, vol. 33, no. 10, pp. 605–610, 2007. DOI: 10.1016/s1553-7250(07)33069-9.

[9] V. Schubert, "Hypotension as a risk factor for the development of pressure sores in elderly subjects," *Age and Ageing*, vol. 20, pp. 255–261, 1991. DOI: 10.1093/ageing/20.4.255.

[10] C. V. Bouten, C. W. Oomens, F. P. Baaijens, and D. L. Bader, "The etiology of pressure ulcers: Skin deep or muscle bound?" *Archives of Physical Medicine and Rehabilitation*, vol. 84, no. 4, pp. 616–619, 2003. DOI: 10.1053/apmr.2003.50038.

[11] E. Landis, "Micro-injection studies of capillary blood pressure in human skin," *Heart*, vol. 15, pp. 209–228, 1930.

[12] C. E. McLennan, M. T. McLennan, and E. M. Landis, "The effect of external pressure on the vascular volume of the forearm and its relation to capillary blood pressure and venous pressure," *Journal of Clinical Investigation*, vol. 21, no. 3, pp. 319–338, 1942. DOI: 10.1172/JCI101306.

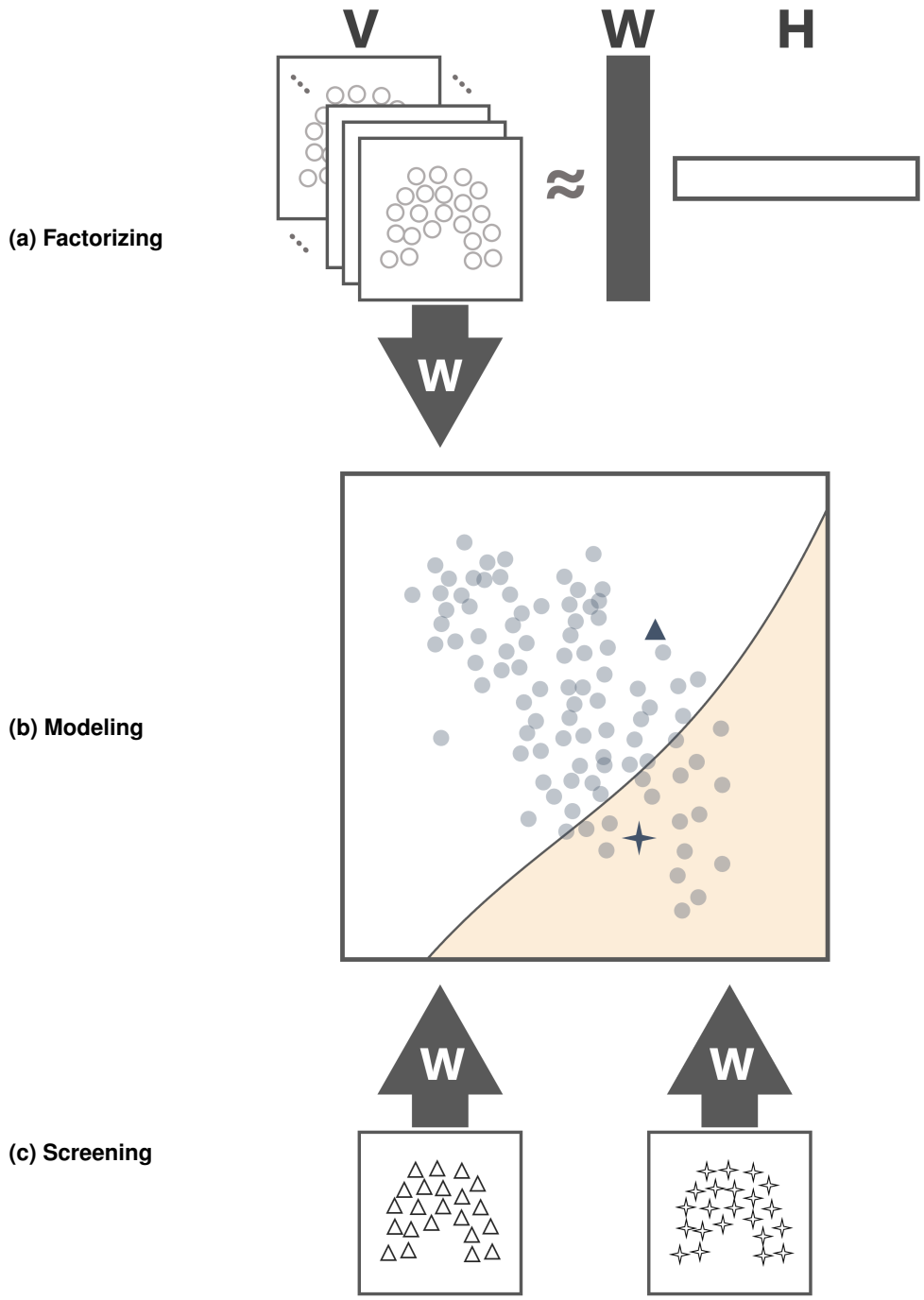

Fig. 7: Computational pipeline for pressure ulcer detection using r-rank nonnegative matrix factorization of training data (a), projection and classification of the training data in the r-dimensional nonnegative feature space (b), and projection and classification of new data in the trained feature space (c).

[13] M. Collier and Z. Moore, "Etiology and risk factors," in *Science and practice of pressure ulcer management*. London: Springer, 2006, ch. 4, pp. 27–36. DOI: 10.1007/1-84628-134-2_4.

[14] Y.-K. Jan and D. M. Brienza, "Technology for pressure ulcer prevention," *Topics in Spinal Cord Injury Rehabilitation*, vol. 11, no. 4, pp. 30–41, 2006. DOI: 10.1310/26R8-UNHJ-DXJ5-XG7W.

[15] D. M. Brienza, P. Karg, M. J. Geyer, S. Kelsey, and E. Trefler, "The relationship between pressure ulcer incidence and buttock-seat cushion interface pressure in at-risk elderly wheelchair users," *Archives of Physical Medicine and Rehabilitation*, vol. 82, pp. 529–533, 2001. DOI: 10.1053/apmr.2001.21854.

[16] S. Sprigle, W. Dunlop, and L. Press, "Reliability of bench tests of interface pressure," *Assistive Technology*, vol. 15, pp. 49–57, 2003. DOI: 10.1080/10400435.2003.10131889.

[17] C.-W. Lung, T. D. Yang, B. A. Crane, J. Elliott, B. E. Dicianno, and Y.-K. Jan, "Investigation of peak pressure index parameters for people with spinal cord injury using wheelchair tilt-in-space and recline: Methodology and preliminary report," *BioMed Research International*, vol. 2014, p. 508 583, 2014. DOI: 10.1155/2014/508583.

[18] M. Wininger and B. Crane, "Effect of interpolation on parameters extracted from seating interface pressure arrays," *Journal of Rehabilitation Research and Development*, vol. 51, no. 9, pp. 1365–1375, 2014. DOI: 10.1682/JRRD.2014.04.0101.

[19] G. DeJong et al., "Factors associated with pressure ulcer risk in spinal cord injury rehabilitation," *American Journal of Physical Medicine and Rehabilitation*, vol. 93, no. 11, pp. 971–986, 2014. DOI: 10.1097/PHM.0000000000000117.

[20] J. Black et al., "National Pressure Ulcer Advisory Panel's updated pressure ulcer staging system," *Advances in Skin and Wound Care*, vol. 20, no. 5, pp. 269–274, 2007. DOI: 10.1097/01.ASW.0000269314.23015.e9.

[21] L. L. Saunders, J. S. Krause, B. A. Peters, and K. S. Reed, "The relationship of pressure ulcers, race, and socioeconomic conditions after spinal cord injury," *Journal of Spinal Cord Medicine*, vol. 33, no. 4, pp. 387–395, 2010. DOI: 10.1080/10790268.2010.11689717.

[22] Tekscan, Inc., *CONFORMat system (Model 5330) [Apparatus]*, 2010.

[23] Permobil, Inc., *Power wheelchair (Model C300) [Apparatus]*, 2005.

[24] Y.-K. Jan, B. A. Crane, F. Liao, J. A. Woods, and W. J. Ennis, "Comparison of muscle and skin perfusion over the ischial tuberosities in response to wheelchair tilt-in-space and recline angles in people with spinal cord injury," *Archives of Physical Medicine and Rehabilitation*, vol. 94, no. 10, pp. 1990–1996, 2013. DOI: 10.1016/j.apmr.2013.03.027.

[25] Y.-K. Jan, F. Liao, M. A. Jones, L. A. Rice, and T. Tisdell, "Effect of durations of wheelchair tilt-in-space and recline on skin perfusion over the ischial tuberosity in people with spinal cord injury," *Archives of Physical Medicine and Rehabilitation*, vol. 94, no. 4, pp. 667–672, 2013. DOI: 10.1016/j.apmr.2012.11.019.

[26] Y.-K. Jan and B. A. Crane, "Wheelchair tilt-in-space and recline does not reduce sacral skin perfusion as changing from the upright to the tilted and reclined position in people with spinal cord injury," *Archives of Physical Medicine and Rehabilitation*, vol. 94, no. 6, pp. 1207–1210, 2013. DOI: 10.1016/j.apmr.2013.01.004.

[27] Y.-K. Jan, M. A. Jones, M. H. Rabadi, R. D. Foreman, and A. Thiessen, "Effect of wheelchair tilt-in-space and recline angles on skin perfusion over the ischial tuberosity in people with spinal cord injury," *Archives of Physical Medicine and Rehabilitation*, vol. 91, no. 11, pp. 1758–1764, 2010. DOI: 10.1016/j.apmr.2010.07.227.

[28] C. L. Maurer and S. Sprigle, "Effect of seat inclination on seated pressures of individuals with spinal cord injury," *Physical Therapy*, vol. 84, pp. 255–261, 2004. DOI: 10.1093/ptj/84.3.255.

[29] F. Pedregosa et al., "Scikit-learn: Machine learning in Python," *Journal of Machine Learning Research*, vol. 12, pp. 2825–2830, 2011. DOI: 10.48550/arXiv.1201.0490.

[30] C. Boutsidis and E. Gallopoulos, "SVD-based initialization: A head start for nonnegative matrix factorization," *Pattern Recognition*, vol. 41, no. 4, pp. 1350–1362, 2008. DOI: 10.1016/j.patcog.2007.09.010.

[31] A. Cichocki and A.-H. Phan, "Fast local algorithms for large scale nonnegative matrix and tensor factorizations," *IEICE Transactions on Fundamentals of Electronics, Communications and Computer Sciences*, vol. E92-A, no. 3, pp. 708–721, 2009. DOI: 10.1587/transfun.E92.A.708.

[32] T. Zhang, "Solving large scale linear prediction problems using stochastic gradient descent algorithms," in *Proceedings of the 21st International Conference on Machine Learning (ICML)*, 2014, p. 116. DOI: 10.1145/1015330.1015332.

[33] D. W. Byrne and C. A. Salzberg, "Major risk factors for pressure ulcers in the spinal cord disabled: A literature review," *Spinal Cord*, vol. 34, no. 5, pp. 255–263, 1996. DOI: 10.1038/sc.1996.46.

[34] J. Reenalda, M. Jannink, M. Nederhand, and M. IJzerman, "Clinical use of interface pressure to predict pressure ulcer development: A systematic review," *Assistive Technology*, vol. 21, no. 2, pp. 76–85, 2009. DOI: 10.1080/10400430903050437.

[35] D. Drummond, A. L. Breed, and R. Narechania, "Relationship of spine deformity and pelvic obliquity on sitting pressure distributions and decubitus ulceration," *Journal of Pediatric Orthopedics*, vol. 5, no. 4, pp. 396–402, 1985. DOI: 10.1097/01241398-198507000-00002.

[36] T. A. Conine, C. Hershler, D. Daechsel, C. Peel, and A. Pearson, "Pressure ulcer prophylaxis in elderly patients using polyurethane foam or jay wheelchair cushions," *International Journal of Rehabilitation Research*, vol. 17, no. 2, pp. 123–137, 1994. DOI: 10.1097/00004356-199406000-00003.

[37] M. J. Rosenthal, R. M. Felton, A. E. Nastasi, B. D. Naliboff, J. Harker, and J. H. Navach, "Healing of advanced pressure ulcers by a generic total contact seat: Two randomized comparisons with low air loss bed treatments," *Archives of Physical Medicine and Rehabilitation*, vol. 84, no. 12, pp. 1733–1742, 2003. DOI: 10.1016/s0003-9993(03)00435-0.

[38] M. Stinson et al., "Spinal cord injury and pressure ulcer prevention: Using functional activity in pressure relief," *Nursing Research and Practice*, vol. 2013, p. 860 396, 2013. DOI: 10.1155/2013/860396.

[39] E. M. Giesbrecht, K. D. Ethans, and D. Staley, "Measuring the effect of incremental angles of wheelchair tilt on interface pressure among individuals with spinal cord injury," *Spinal Cord*, vol. 49, no. 7, pp. 827–831, 2011. DOI: 10.1038/sc.2010.194.

[40] Y. Chen, J. Wang, C.-W. Lung, T. D. Yang, B. A. Crane, and Y.-K. Jan, "Effect of tilt and recline on ischial and coccygeal interface pressures in people with spinal cord injury," *American Journal of Physical Medicine and Rehabilitation*, vol. 93, no. 12, pp. 1019–1030, 2014. DOI: 10.1097/PHM.0000000000000225.

[41] M. Kosiak, "Etiology and pathology of ischemic ulcers," *Archives of Physical Medicine and Rehabilitation*, vol. 40, pp. 62–69, 1959.

[42] Y.-K. Jan, D. M. Brienza, M. L. Boninger, and G. Brenes, "Comparison of skin perfusion response with alternating and constant pressures in people with spinal cord injury," *Spinal Cord*, vol. 49, no. 1, pp. 136–141, 2011. DOI: 10.1038/sc.2010.58.

[43] Y.-K. Jan, D. M. Brienza, M. J. Geyer, and P. Karg, "Wavelet-based spectrum analysis of sacral skin blood flow response to alternating pressure," *Archives of Physical Medicine and Rehabilitation*, vol. 89, no. 1, pp. 137–145, 2008. DOI: 10.1016/j.apmr.2007.07.046.

[44] M. Law, ""Opportunistic" screening," *Journal of Medical Screening*, vol. 1, no. 4, p. 208, 1994. DOI: 10.1177/096914139400100403.

[45] R. M. Summers et al., "Feasibility of simultaneous computed tomographic colonography and fully automated bone mineral densitometry in a single examination," *Journal of Computer Assisted Tomography*, vol. 35, no. 2, pp. 212–216, 2011. DOI: 10.1097/RCT.0b013e3182032537.

[46] D. Ding et al., "Usage of tilt-in-space, recline, and elevation seating functions in natural environment of wheelchair users," *Journal of Rehabilitation Research and Development*, vol. 45, no. 7, pp. 973–984, 2008. DOI: 10.1682/jrrd.2007.11.0178.

[47] S. E. Sonenblum and S. Sprigle, "Distinct tilting behaviours with power tilt-in-space systems," *Disability and Rehabilitation: Assistive Technology*, vol. 6, no. 6, pp. 526–535, 2011. DOI: 10.3109/17483107.2011.580900.

[48] T. D. Yang, S. A. Hutchinson, L. A. Rice, K. L. Watkin, and Y.-K. Jan, "Development of a scalable monitoring system for wheelchair tilt-in-space usage," *International Journal of Physical Medicine and Rehabilitation*, vol. 1, no. 4, p. 129, 2013. DOI: 10.4172/2329-9096.1000129.

[49] R. Dai, S. E. Sonenblum, and S. Sprigle, "A robust wheelchair pressure relief monitoring system," in *2012 Annual Conference of the IEEE Engineering in Medicine and Biology Society (EMBC)*, 2012, pp. 6107–6110. DOI: 10.1109/EMBC.2012.6347387.

[50] E. Marenzi, G. M. Bertolotti, and A. Cristiani, "Design and development of a monitoring system for the interface pressure measurement of seated people," *IEEE Transactions on Instrumentation and Measurement*, vol. 62, no. 3, pp. 570–577, 2013. DOI: 10.1109/TIM.2013.2240051.

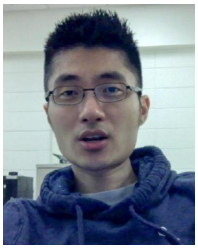

Tim D. Yang is a PhD candidate in kinesiology at the University of Illinois Urbana-Champaign. As part of the Program in Computational Science and Engineering, he applies his background in computer science toward developing smart technologies for people with disabilities. His doctoral research focuses on computational rehabilitation for power seating and mobility.

Yih-Kuen Jan is Associate Professor and Director of the Rehabilitation Engineering Lab at the University of Illinois Urbana-Champaign. He received his PhD in rehabilitation science and technology at the University of Pittsburgh in 2004. His research focuses on assistive technology, adaptive sports, and soft tissue biomechanics.